Hysteresis loops of magnetic thin films with perpendicular anisotropy

E. A. Jagla
Centro Atómico Bariloche and Instituto Balseiro, (8400) Bariloche, Argentina
(Received 3 February 2005; revised manuscript received 31 May 2005; published 8 September 2005)

We model the magnetization of quasi-two-dimensional systems with easy perpendicular (z) axis anisotropy upon change of the external magnetic field along z. The model is a generalization of the scalar "phi-fourth" model that considers only the z component of the magnetization, and includes magnetic exchange, dipolar interactions, structural disorder, and an external z-oriented magnetic field. The phase diagram in the disorder/interaction strength plane is presented, and the different qualitative regimes are analyzed, mainly focusing on the existence or not of an abrupt nucleation step in the process of magnetization reversal. The results compare very well with observed experimental hysteresis loops and spatial magnetization patterns, as for instance in the case of Co-Pt multilayers.

DOI: 10.1103/PhysRevB.72.094406 PACS number(s): 75.60.−d, 75.70.Cn, 75.10.Hk

I. INTRODUCTION

The detailed understanding of the phenomena responsible for magnetic hysteresis[1,2] is of great importance in theoretical and applied considerations, as for instance in the magnetic recording technology.[3] Magnetic hysteresis originates in the existence of different metastable configurations compatible with the same value of the applied external field. When the external field is changed, the system adapts by finding the nearest metastable minimum in configuration space. During this process energy is dissipated, and upon a sweep of the external field this manifests in a nonvanishing hysteresis loop, whose area is related to the energy dissipated during the process. In this description of hysteresis the external field is assumed to change infinitely slowly, in such a way that the system adapts in every moment to the actual value of the external field. However, in general this is not enough to guarantee a smooth evolution of the microscopic degrees of freedom of the system, and that is the origin of dissipation and hysteresis.

Although the qualitative origin of hysteresis is well understood, a completely different issue is to reproduce in detail the observed hysteretic behavior of real systems. This is particularly true when competing interactions make the energy landscape of the system have many different metastable minima. Typical competing interaction terms are the magnetic exchange favoring a parallel alignment of the magnetization, and the dipolar term which favors an antiparallel arrangement in a plane perpendicular to the magnetization.

In the present paper we model the hysteretic behavior of thin magnetic films with perpendicular anisotropy. These systems are promising as high density magnetic storage media,[4] and they are receiving a great deal of experimental attention.[5–8] In particular, the effect of the disorder on the shape of the hysteresis loops and magnetization configurations has started to be analyzed.[6–8]

The paper is divided as follows. In Sec. II we discuss the scalar model we use, which is appropriate for the present case where magnetization points almost everywhere in the perpendicular direction. Section III contains the results of the numerical simulations, and in Sec. IV we compare the results with experimental data in Co-Pt multilayers and conclude.

II. DEFINITION OF THE MODEL

Magnetism originates in quantum effects occurring at the atomic level. To model macroscopic hysteresis, however, it is impossible in practice to start from these elemental building blocks in order to arrive to the macroscopic description. The *micromagnetic approach*[1,2] starts from an intermediate scale description, in which the magnetic moment $\mathbf{m}$ of an elemental piece of material is taken as the fundamental variable. $\mathbf{m}$ is a vector field, which is a function of the spatial coordinates and time, and it is assumed to satisfy at any position and time the constrain $|\mathbf{m}|^2=1$, where a rescaling of the amplitude has been assumed. A reasonably detailed description of magnetization evolution is provided by the phenomenological Landau-Lifshitz-Gilbert (LLG) equation,[1,2,9] that can be written as

$$\frac{\partial \mathbf{m}}{\partial t} = -a\mathbf{m}\times\mathbf{B} - b\mathbf{m}\times(\mathbf{m}\times\mathbf{B}), \tag{1}$$

where $\mathbf{B}$ is the local effective magnetic field. The first term on the right of Eq. (1) describes a precessional evolution of $\mathbf{m}$ around $\mathbf{B}$, and the second term is a phenomenological damping term that tends to align $\mathbf{m}$ with $\mathbf{B}$. Note that from this equation we obtain immediately that $\partial|\mathbf{m}|^2/\partial t=0$, i.e., it automatically maintains the norm of $\mathbf{m}$ as fixed. In equilibrium ($\partial\mathbf{m}/\partial t=0$), this equation reduces to Brown's equation,[1,2] namely $\mathbf{m}\times\mathbf{B}=0$, stating that at any point the local magnetization has to be aligned with the local field. The local field $\mathbf{B}$ includes contributions from the external applied field, from the interaction with all the rest of the magnetic moments in the sample, and from structural anisotropies in the sample.

Equation (1) is a sufficiently detailed starting point to obtain the time and space evolution of the magnetization. Unfortunately, it is frequently a too much detailed starting point. In fact, except in simple cases, the vectorial nature of $\mathbf{m}$ and the different temporal scales for precessional and relaxation effects makes the numerical solution of Eq. (1) extremely demanding.[10]

For the problem we want to study a much simpler formulation is possible. The main point is to recognize that at every

moment, the local magnetization in the sample points almost everywhere in the z direction. The only exception are domain walls, where the z component of magnetization changes sign continuously. Experimental results show[6–8] that in the systems we are trying to model, these domain walls have a width which is much smaller than the size of the regions in which magnetization remains uniform. We are interested in the spatial distribution of magnetization, and not in the detailed internal structure of domain walls, and this is what makes it possible to work with a scalar model in terms of m_z only.

In fact, models of this type have been widely used in the past. A convenient starting point is the "dipolar phi-fourth" model, described by the dynamical equation[11–13]

$$\frac{\partial \phi(\mathbf{r})}{\partial t} = h_0 - A(-\phi + \phi^3) - \gamma \int d\mathbf{r}' \frac{\phi(\mathbf{r}')}{(|\mathbf{r}-\mathbf{r}'|^3)} + J\nabla^2\phi. \tag{2}$$

The scalar variable ϕ (which may be assimilated to the z component of the local magnetization) evolves in a local two-well potential [the A-proportional term in Eq. (2)] which mimics the existence of two privileged values (± 1) for ϕ. h_0 is the external field and the last two terms are the dipolar and exchange contributions, respectively. The form of the exchange term is just the simplest form that produces a finite energy for a domain wall. Since in our description we do not intend to describe domain walls in more detail, this form is enough for our purposes. We have used this model previously[13] to study magnetization patterns in magnetic garnets and ferrofluids. This is essentially the kind of model we are going to use here, but some modification is necessary to correct for some nonphysical feature of Eq. (2) concerning the global magnetization: In Eq. (2), $|\phi|$ is not restricted to be bounded, and, in fact, arbitrarily large values of ϕ are obtained if the external field is strong enough. This unrealistic behavior has to be cured if we want to reproduce the form of macroscopic hysteresis loops, where saturation does occur. There is a very simple and natural modification of Eq. (2) which provides magnetization saturation. In fact, consider an isolated magnetic moment in the presence of a field pointing in the z direction of amplitude B (which may even be time dependent). According to the complete equation (1), the z component of the magnetization evolves according to

$$\frac{dm_z}{dt} = b(1-m_z^2)B \tag{3}$$

and this equation, of course, predicts that $|m_z|$ will never overpass the value 1. It is immediate to implement this prescription in a model like that of Eq. (2), by modifying it to the form

$$\frac{\partial \phi(\mathbf{r})}{\partial t} = (1-\phi^2)B + J\nabla^2\phi \tag{4}$$

with

$$B = h_0 + A\phi - \gamma \int d\mathbf{r}' \frac{\phi(\mathbf{r}')}{(|\mathbf{r}-\mathbf{r}'|^3)}. \tag{5}$$

Note that we have set the constant b to 1 by appropriately redefining J and the time unit. Different terms on the right hand side of Eq. (5) represent, respectively, the external field, the local anisotropy (taken to lowest order)[1,2] and the dipolar interaction.

We also want to take into account in the model the existence of structural disorder, which can nowadays be introduced in a controlled manner in the experiments.[6,7] In this respect, it is worth mentioning the previous work on the random field Ising model (RFIM) introduced by Sethna *et al.*[14] This is a generalization of the Ising model (with nearest neighbor couplings, no dipolar interactions) where a quenched random field is assumed to be present at every site. This is an important model system, where the effect of disorder on the existence or not of an abrupt nucleation step in the process of magnetization reversal was analyzed in detail. The RFIM is a good prototypical model, but from an experimental point of view, the existence of quenched random fields in different positions of the sample is difficult to justify, as it implies a breaking of the time reversal symmetry. Other people[15] suggested that it would be more physical to introduce disorder in the strength of the bonds of the Ising model (random bond), in the direction of the easy axis for the magnetization (random anisotropy), or in the value of the coercive field that has to be applied to revert a single spin (random coercivity Ising model). In our model given by Eqs. (4) and (5), it is very simple to introduce disorder in the parameter A. As we said, this parameter controls the strength of the anisotropy energy in the system. Note also that it is a measure of the coercive field necessary to revert an isolated spin: a spin will be locally in equilibrium if it points in the direction of the local field. We see that $m_z=+1$ ($m_z=-1$) is an equilibrium configuration of that spin if $h_0+A>0$ ($h_0-A<0$). Then A represents the value of the local coercive field that is necessary to apply in order to invert the orientation of the spin. We will choose the value of A to vary spatially according to

$$A(\mathbf{r}) = A_0[1 + D\eta(\mathbf{r})], \tag{6}$$

where η is a spatially random and uncorrelated Gaussian variable, with zero mean and unitary variance (η is cut off at large negative values, namely $\eta > -1/D$, to guarantee $A>0$). D controls the overall intensity of disorder.

We want to make a comment about the use of a continuous variable to describe the z axis magnetization. It seems that for our purposes a discrete ± 1 variable would suffice. This is true in principle, but there is a technical problem in using a ± 1 variable: if the fundamental variables take only two values, domain walls are forced to be one lattice parameter thick. This produces domain walls that are artificially pinned to the numerical lattice, and this makes realistic simulations of homogeneous and isotropic systems very difficult.[16]

To close this section, we want to comment about a subtle point concerning the inversion symmetry in spin space of the problem. The time evolution equations of our model [Eqs.

(4) and (5)] do not change upon the inversion of all spins and the external field ($\{\phi,h_0\}\rightarrow\{-\phi,-h_0\}$). However, the full LLG Eq. (1) does not possess this symmetry. In a certain sense, in passing from the full LLG equation to a scalar description, we are averaging out the precession of spins, and this may imply that we are not describing some dynamical symmetry breaking effects that can in principle be present. This point has been recently emphasized by Deutsch and Mai.[10] It seems that this kind of effect, if present, does not show up at the level of the results we are going to present in the rest of this paper.

III. RESULTS

The model simulated is thus given by Eqs. (4) and (5), with the disorder function $A(\mathbf{r})$ given by Eq. (6). The results presented below correspond to zero temperature. Thus the evolution of the system is driven exclusively by the tendency to minimize the energy. We will see that even this $T=0$ case is very rich, and provides different macroscopic forms of the hysteresis curve when the interaction strength between spins and the amount of structural disorder are changed. The results obtained compare very well with experimental results.

The parameters of the model are A_0, D, γ, and J, in addition to the external field h_0. As explained in Ref. 9, the ratio between J and γ can be adjusted by appropriately rescaling the spatial scale in the model. In the simulations below we choose $\gamma=0.095\ J$, and give the results in term of h_0/A_0, J/A_0, and D. The mesh parameter is taken as the unit of length.

For each set of parameters we start with a very high value of h_0, where the system is fully polarized, and start decreasing h_0 in small steps. At each step the simulation is run until full convergence is achieved, and then the spatial distribution of magnetization is examined, and the global magnetization m is calculated as the spatial average of ϕ. The main result we are going to present is the disorder-exchange/anisotropy ratio ($D-J/A_0$) phase diagram of the model, and its description. The phase diagram is presented in Fig. 1. The form of the hysteresis loop at different positions is shown in Fig. 2.

For large J/A_0, ($2.1\lesssim J/A_0$) the system shows no hysteresis at all. A closer examination of the magnetization distribution shows that in this region the interaction is so strong that effectively, the two minima of the local magnetization disappear, and ϕ remains almost uniform in the sample, changing smoothly as a function of the applied field. This regime is certainly outside the region in which the model is justified, and then we will not consider it.

More interesting to us is the rest of the phase diagram, where hysteresis occurs, and where (from the examination of magnetization distribution) we observe well defined domains with magnetization ±1. That is the part plotted in Fig. 1. Two main regions can be defined here. They correspond to the existence or not of a finite magnetization jump upon field variation. On the basis of the results for the simulated points in the phase diagram (some additional simulated points are not shown), we can infer the existence of a line (sketched by the continuous line) separating a region in which a finite magnetization jump occurs (at the left of this line) or does not occur (at the right of this line). In addition, if a jump exists, it can lead directly to the fully inverted magnetization state, or to a partial inversion, that requires a further change of the external field to completely revert the magnetization. These two possibilities are separated by a different line,

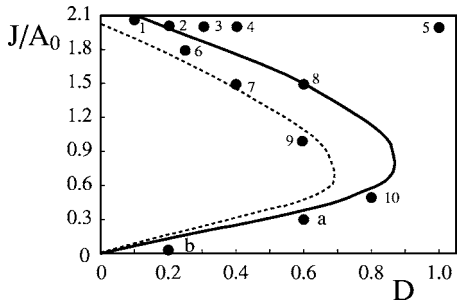

FIG. 1. Disorder-exchange/anisotropy ratio ($D-J/A_0$) phase diagram for the model described by Eq. (4), in a system of size 384×384, with $\gamma=0.095\ J$. Numbers indicate the points for which the hysteresis loops are shown in the next figure. The continuous line is the main feature of the diagram, separating regions in which an abrupt nucleation event occurs (to the left of this line) or not (to the right). In addition, the nucleation event produces complete magnetization reversal to the left of the dotted line, but only partial magnetization reversal between this curve and the continuous line (the location of the lines is only approximate, based on the results for the indicated points, and some others not shown).

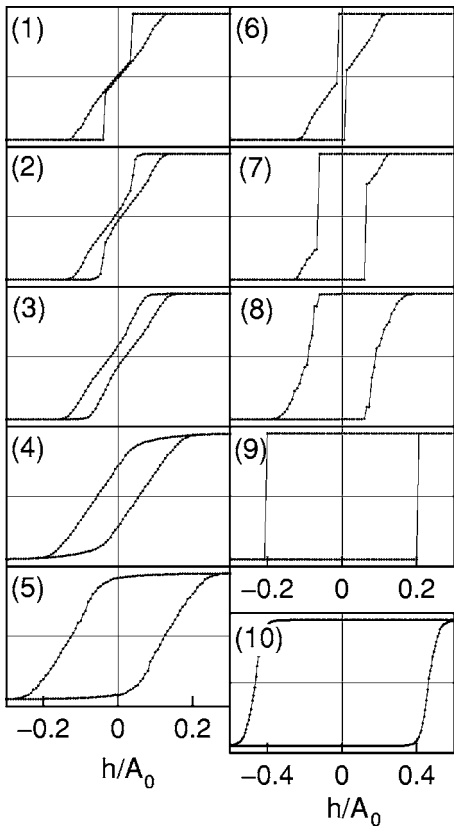

FIG. 2. The hysteresis loops at different locations of the phase diagram shown in the preceding figure. In the vertical axis we plot the z-axis magnetization, which changes between ±1 as the field is changed.

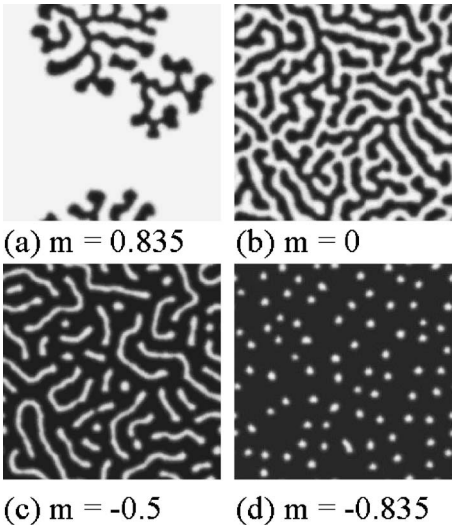

FIG. 3. Four snapshots of the spatial magnetization distribution corresponding to hysteresis loop (1) in Fig 2. The values of the magnetization at which the snapshot were taken are indicated. Note that the first panel is an unstable configuration, which is spontaneously evolving toward a state with $m \simeq 0.3$ (in this and following figures, the gray scale from black to white represents magnetization values ranging from −1 to +1).

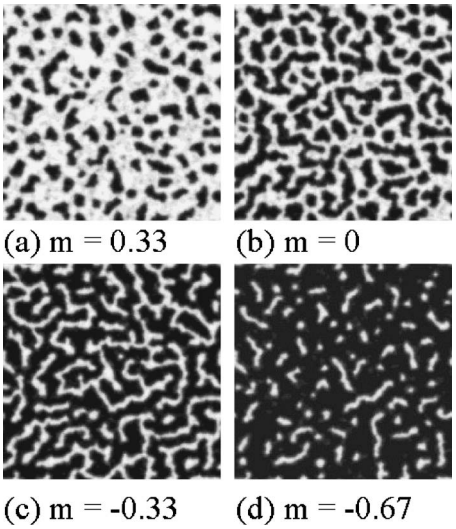

FIG. 4. Same as Fig. 3, for hysteresis loop (4) in Fig 2.

sketched as a dotted line in Fig. 1. A magnetization jump indicates an instability in the system, in which a finite fraction of the spins change their orientations, upon an infinitesimal change of the external field. This avalanche process in magnetic systems was originally analyzed in the RFIM.[14] It was shown that if disorder in the system is lower than some critical amount, then there is a magnetization jump, whereas there is no jump for higher disorder. The same result is qualitatively obtained here, the amplitude of the magnetization jump vanishes continuously when we approach the continuous line from the left in Fig. 1. This line is a critical line, in the same sense used in the RFIM. We expect that the vanishing of the abrupt jump follows a power law close to the critical line. However, we have not attempted to determine critical exponents since in the presence of the dipolar interaction we cannot go to system sizes large enough to get good statistics. An interesting question that remains open is whether the critical exponents are the same all along the critical line or not.

The spatial distribution of magnetization shows characteristic features for different forms of the hysteresis loops. Examples are shown in Figs. 3–7, corresponding to hysteresis loops (1), (4), (9), (7), and (10) in Fig. 2. Figure 3 corresponds to a case where there is an abrupt nucleation, leading to a partially inverted magnetization state. Panel (a) in Fig. 3 is a *nonequilibrium* configuration after the nucleation. The final state at this field corresponds to a configuration of magnetization ~0.3. Further decrease of the field [panels (c) and (d)] is necessary to completely invert the magnetization. In the presence of strong disorder, for approximately the same value of J/A_0 (Fig. 4) the nucleation step is smoothed, and the whole evolution is continuous. Here disorder plays a fundamental role in preventing the spontaneous growth of the nucleated domains, which in this case remain pinned by the structural disorder, and need a further decrease of the field to be able to grow.

Figure 5 displays a case in which the nucleation event takes the sample in the opposite fully magnetized state. Note how in this case, the domain that nucleates is a rather featureless, more or less circular object, and grows to take over the whole sample. This case has to be compared with Fig. 3, in which the domains nucleated maintain a striped internal structure. An intermediate case is that of Fig. 6. Here the inverted magnetization bubble almost invades the whole sample at once. However, a small fraction of domains with the original orientation remains. This is reflected in the form of the magnetization loop, which in fact shows an abrupt jump of the magnetization from +1 to about −0.5.

The last case (Fig. 7) corresponds to a weakly interacting sample (lower value of J/A_0). However, the disorder is sufficiently strong to avoid a sudden nucleation step. We see the

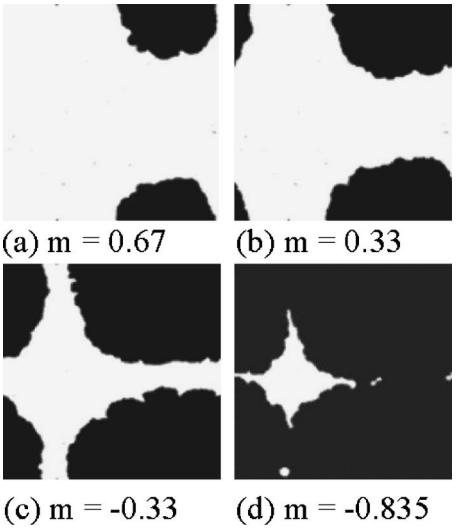

FIG. 5. Same as Fig. 3, for hysteresis loop (9) in Fig. 2. None of these configurations is stable, they are spontaneously evolving to the completely inverted magnetization state.

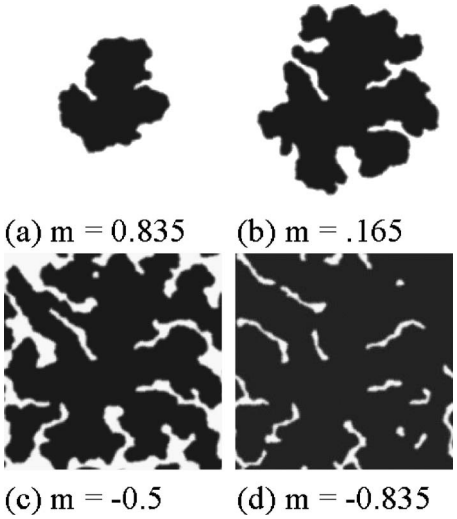

FIG. 6. Same as Fig. 3, for hysteresis loop (7) in Fig. 2. The first two panels show the spontaneous growth of the nucleated domain.

different configuration of the domains in this case, which do not show the typical striped pattern of the other cases (originated in the dipolar interaction) but patterns mainly dominated by the disorder. This case, in which the dipolar interaction plays a minor role, is qualitatively similar to that studied in the RFIM.

One striking characteristic of the phase diagram we are presenting is the re-entrance of the sector with continuous hysteresis. This re-entrance tells that if D is not too high, samples displaying continuous hysteresis can be classified in two well different groups: weakly interacting ones for low J/A_0, and strongly interacting ones for large J/A_0. For strongly interacting samples, the width of the hysteresis loop (measured as the distance between the two branches, at a fixed magnetization) can be much smaller than the change of magnetic field necessary for complete magnetization inversion [see for instance loop (3) in Fig. 2]. In these samples the coercive field is much lower than the saturation field, and remanent magnetization is much lower than saturation magnetization.

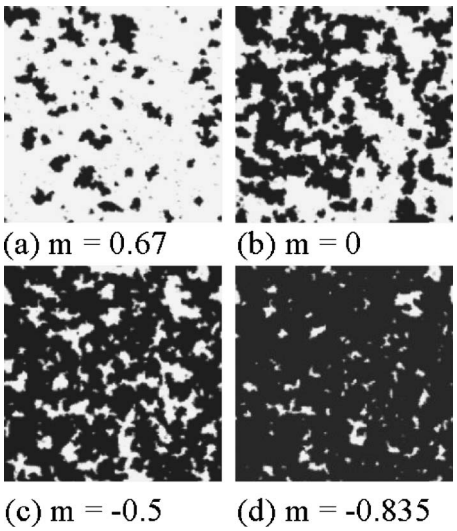

FIG. 7. Same as Fig. 3, for hysteresis loop (10) in Fig. 2.

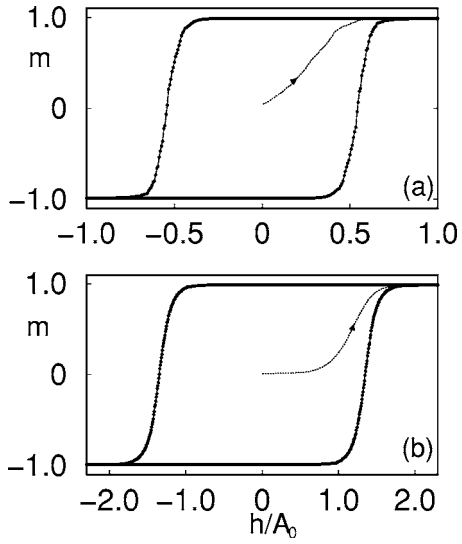

FIG. 8. Hysteresis loops and virgin curves, obtained from a demagnetized sate, showing two different qualitative cases: a "nucleation dominated" magnet (a) in which the initial permeability of the sample is rather large, and a "pinning dominated" magnet (b), with a small initial permeability (the parameters in both cases correspond to those of points labeled "a"and "b" in Fig. 1). Note that the two cases correspond to what we have called weakly interacting samples.

In weakly interacting samples the range of external field on which the complete magnetization inversion occurs is small compared with the width of the hysteresis loop [as for instance in loop (10) in Fig. 2]. As a consequence, these samples possess a coercive field which is of the order of the saturation field. In addition, the remanent magnetization is essentially the saturation magnetization.

The case of what we have called "weakly interacting samples" allows yet a further distinction, which however cannot be inferred from the results shown up to now only. In fact, weakly interacting samples are examples of "permanent magnets." A usual distinction among permanent magnets is made between nucleation type magnets and pinning type magnets.[2] They are phenomenologically distinguished by the form of the virgin magnetization curve. Pinning type magnets display a small initial permeability at the demagnetized state, whereas for nucleation type magnets the initial permeability is very large. The two different behaviors can be obtained with the present model. An example is shown in Fig. 8 (for simplicity in the simulation, we obtain a demagnetized system by *quenching* from a high temperature configuration, instead of the *annealing* process usually invoked). Pinning type magnets are modeled through a very low value of the interaction. The system behaves essentially as a collection of isolated magnetic moments, that switch in the presence of the external field at the particular value of the local coercive field. The transition is seen to be smoothed because of broad distribution of local coercive fields. For larger values of the interaction strength (but still in the region corresponding to weakly interacting samples) we can see how the initial permeability increases noticeable. Here, domain walls (which are abundant in the demagnetized state) have some freedom

to move in the presence of the external field, and this produces a high permeability. However, once fully magnetized and upon inversion of the external field, domains with opposite magnetization have to be nucleated, and this requires much larger fields. Note how the difference in the two virgin curves occur in two samples that have a very similar shape of the full hysteresis loop.

IV. COMPARISON WITH EXPERIMENTS AND CONCLUSIONS

There has been in recent years much interest in the behavior of thin multilayer magnetic films,[5–8] mainly as potential high density magnetic storage media. Particular attention is being paid to Co-Pt multilayers. The influence of disorder on these materials has only recently started to be studied systematically. An example of the evolution of hysteresis loops upon change of the structural disordered in the sample is contained in Ref. 12. There, Co-Pt multilayers were grown under different values of argon sputtering pressure, what allows for the introduction of disorder in a controlled way. We can compare the plots in Fig. 1 of Ref. 12 with the hysteresis loops of the present model for a value $J/A_0 \simeq 2$ [see panels (1) to (5) in Fig. 2] in which the disordered is progressively increased. The qualitative agreement between the model and the experiment is very good, taking into account the simplifications in the model. Comparison of our results with images from magnetic scattering techniques (Fig. 2 in Ref. 12, for instance) reveals also that even the real space configurations are quite realistic. We see that the samples analyzed in Refs. 11 and 12 fit very well in the strong interaction region of our phase diagram.

The relevance of the present results to experiments is twofold. On one side, it gives insight on the main physical ingredients that have to be considered to obtain a thorough description of the phenomena. On the other side, it is also important in the following sense. In many cases, experimental information of the real space patterns is inferred from observation of the x-ray diffraction patterns, in which only the amplitude information is conserved. Then the conclusions drawn from the experiments depend on the possibility of extracting information of the real space patterns from the x-ray patterns, and this is not a trivial issue. The present model, providing directly the configuration in real space (which can of course be transformed to get the x-ray patterns) is an ideal benchmark in which the x-ray reconstruction techniques can be tested. A more detailed statistical comparison between simulated and measured patterns along these lines will be published elsewhere.

ACKNOWLEDGMENTS

I am indebted to Larry Sorensen, Michael Pierce, and Conor Buechler for persuading me to do simulations including disorder, and for many exciting discussions and comments. I also thank Josh Deutsch for fruitful discussions.

[1] G. Bertotti, *Hysteresis in Magnetism* (Academic Press, San Diego, 1998).

[2] A. Hubert and R. Schäfer, *Magnetic Domains* (Springer-Verlag, Berlin, 1998).

[3] A. Moser, K. Takano, D. T. Margulies, M. Albrecht, Y. Sonobe, Y. Ikeda, S. Sun, and E. E. Fullerton, J. Phys. D **35**, R157 (2002); K. Okuchi, IEEE Trans. Magn. **37** 1217 (2001); J. I. Martín, J. Nogués, K. Liu, J. L. Vicent, and I. K. Schuller, J. Magn. Magn. Mater. **256**, 449 (2003).

[4] S.-I. Iwasaki, IEEE Trans. Magn. **20**, 657 (1984); W. Cain, A. Payne, M. Baldwinson, and R. Hempstead, *ibid.* **32**, 97 (1996).

[5] E. E. Fullerton, J. Pearson, C. H. Sowers, S. D. Bader, X. Z. Wu, and S. K. Sinha, Phys. Rev. B **48**, 17432 (1993); J. H. Kim and S. C. Shin, J. Appl. Phys. **80**, 3121 (1996); J. B. Kortright, S. K. Kim, G. P. Denbeaux, G. Zeltzer, K. Takano, and E. E. Fullerton, Phys. Rev. B **64**, 092401 (2001); O. Donzelli, D. Palmeri, L. Musa, F. Casoli, F. Albertini, L. Pareti, and G. Turilli, J. Appl. Phys. **93**, 9908 (2003); D. L. Mobley, C. R. Pike, J. E. Davies, D. L. Cox, and R. R. P. Singh, J. Phys.: Condens. Matter **16**, 5897 (2004).

[6] M. S. Pierce, R. G. Moore, L. B. Sorensen, S. D. Kevan, O. Hellwig, E. E. Fullerton, and J. B. Kortright, Phys. Rev. Lett. **90**, 175502 (2003).

[7] M. S. Pierce, C. R. Buechler, L. B. Sorensen, J. J. Turner, S. D. Kevan, E. A. Jagla, J. M. Deutsch, T. Mai, O. Narayan, J. E. Davies, K. Liu, J. H. Dunn, K. M. Chesnel, J. B. Kortright, O. Hellwig, and E. E. Fullerton, Phys. Rev. Lett. **94**, 017202 (2005).

[8] J. E. Davies, O. Hellwig, E. E. Fullerton, G. Denbeaux, J. B. Kortright, and K. Liu, Phys. Rev. B **70**, 224434 (2004).

[9] L. D. Landau, E. M. Lifshitz, and L. P. Pitaevski, *Statistical Physics*, Part 2 (Pergamon, Oxford, 1980); T. L. Gilbert, Phys. Rev. **100**, 1243 (1955).

[10] J. M. Deutsch and T. Mai, Phys. Rev. E **72**, 016115 (2005).

[11] M. Seul and D. Andelman, Science **267**, 476 (1995); F. Elias, C. Flament, J.-C. Bacri, and S. Neveu, J. Phys. I **7**, 711 (1997).

[12] C. Sagui and R. C. Desai, Phys. Rev. Lett. **71**, 3995 (1993); Phys. Rev. E **49**, 2225 (1994); **52**, 2807 (1995).

[13] E. A. Jagla, Phys. Rev. E **70**, 046204 (2004).

[14] J. P. Sethna, K. Dahmen, S. Kartha, J. A. Krumhansl, B. W. Roberts, and J. D. Shore, Phys. Rev. Lett. **70**, 3347 (1993).

[15] E. Vives and A. Planes, Phys. Rev. B **63**, 134431 (2001); E. Vives and A. Planes, J. Magn. Magn. Mater. **221**, 164 (2000); O. Hovorka and G. Friedman, cond-mat/0306300 (unpublished).

[16] A. Magni, Phys. Rev. B **59**, 985 (1999); A. Magni and G. Vertesy, *ibid.* **61**, 3203 (2000); U. Nowak, U. Rudiger, P. Fumagalli, and G. Guntherodt, *ibid.* **54**, 13017 (1996); U. Nowak, J. Heimel, T. Kleinefeld, and D. Weller, *ibid.* **56**, 8143 (1997).